EDDY CURRENT SEPTUM MAGNETS FOR BOOSTER INJECTION AND EXTRACTION, AND STORAGE RING INJECTION AT SSRF

L. Ouyang, M. Gu, B. Liu, R. Chen, Z. Chen,

Shanghai Institute of Applied Physics, Shanghai 201800, CHINA

Abstract

There are 6 in-vacuum eddy current septum magnets used for Booster injection, extraction, and Storage Ring injection in SSRF. Special attentions were paid to coils and their support design because of the magnetic shock force and the high heat on the coils. For storage ring magnets, good transverse homogeneity in the gap and an extremely low leakage field on the stored beam are their key features. Magnetic field measurement was conducted with both point coil and long integral coil, and the results agreed well with the OPERA-2d/3d simulations. An inner tube is added to keep the continuity of impedance for the circulating beam with RF finger flanges at each end. Sputter ion pumps integrated with NEG are used to acquire the UHV for the chamber.

INTRODUCTION

When beam current with energy of 150 MeV from Linac arrives at the end of LTB transfer line, it will first be deflected by the septum magnet, then kicked onto the booster orbit by the kicker. After the energy is ramped to 3.5 GeV, the beam is extracted by a fast single turn extraction scheme which consists of one kicker, 3 slow kickers (bump magnets), one thin septum magnet and two thick septum magnets.

The injection into the storage ring will be in the horizontal plane by means of two septum magnets and four kickers. This method provides a smooth and continuous injection. The injection efficiency is the main concern of the septum magnets. To this end we rely on good transverse homogeneity in the gap for the injected beam and low leakage field on the circulating beam. Table 1 shows the basic parameters of some of SSRF septum magnets.

Table 1 Basic parameters of booster thick septum magnets and storage ring septum magnets

	Booster	SR
No. of magnets	2	2
Length (m)	0.6	0.8
Deflection angle (mrad)	52.20	55
Magnetic field (Gauss)	10150	8082
Gap height and width (mm)	12×40	12×40
Minimum septum thickness (mm)		<3*
Good field region(mm*mm)	26×10	28×10
Half sine pulse width(μs)	60	60
Repetition rate (Hz)	2	2
Field transverse homogeneity		2%
Leakage field		0.1%

* at injection point

MAGNETS DESIGN AND VACUUM CONSIDERATIONS

The magnetic cores were laminated with steel sheets punched into the U shape with gap height of 12 mm and width of 40 mm. The sheet material (10JNEX900) is non-oriented, double coated, 0.1 mm thick, with high content of silicon. It has a low core loss and high permeability at high frequencies. The core was enclosed by OFHC copper box. Except the ends, all sides of the box were curved into arc shapes with different radii of curvature for booster magnet and storage magnet respectively. For storage ring injection thin septum magnet, the thickness of septum wall was optimized at less than 3 mm at the injection point. A trough with trapezoidal section shape was cut in the septum wall along the circulating beam direction, with the minimum thickness at the injection point.

All the magnets were placed in cylinder vacuum chambers. For storage ring, it is of great importance to preserve the continuity of beam impedance, so an inner tube was added against the trapezoidal trough of the septum wall for the circulating beam (Fig. 1). Both its ends were connected with RF fingers bellows to the other vacuum chamber of storage ring injection straight section. There was no vacuum separation between the inner tube and magnet chamber. A Mumetal sheet of 0.25 mm thick adapted to the outer surface geometry of inner tube forms a shielding screens to further reduce the leakage field.

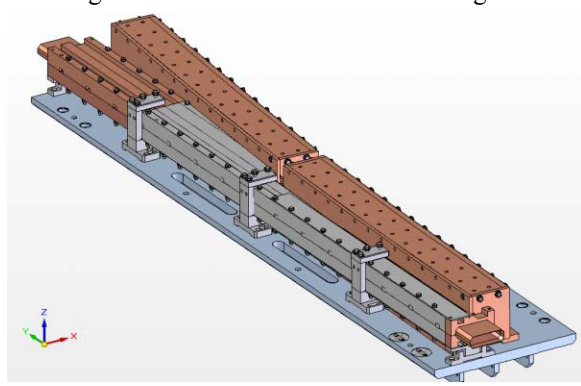

Figure 1: View of the SR septum magnets with inner beam tube.

Because of the huge out-gassing surfaces of the core sheets and the gas entrapment in each magnet, UHV treatments of all materials before the assembly and at least 200°C, 24 hours baking before and after installation were necessary. For the booster magnet chamber, it needs

a vacuum pressure of 5×10^{-6} Pa, which was acquired by using two 400l/s sputter ion pumps. While for the storage ring one, it has higher vacuum pressure (2.6×10^{-8} Pa), so 3 400l/s sputter ion pumps, each integrated with a 400l/s SAES ST707 no evaporable getter (NEG) were used.

COIL DEFORMATION, THERMAL ANALYSIS AND MAGNETIC FIELD ANALYSIS

Coil Deformation Analysis

The coil was made of solid copper bar, and wounded around the back side of the core; its fixation and insulation make use of the machinable ceramics cut into suitable shape and placed in between the steel sheets as spacers to clamp firmly the coil.

For booster extraction magnets, the deflection magnetic field is around 1.0 Tesla, with gap height 12 mm, magnetic core length 600 mm ,the peak value of magnetic force for a 2 Hz 60 us half sine pulse on the coil is 2865 (N). This equals approximately to a pressure of 400000 N/m^2 on the coil in the aperture. The force is on the horizontal plane, and the direction is to inner side of the gap.

ANSYS LS-DYNA explicit finite element program was used for the dynamic analysis of coil deformation. The stress-strain relation is described by bilinear isotropic plasticity model. For copper, the modulus of elasticity is $1.38\times10^{11}N/m^2$, the Poisson's ratio 0.36, yield stress $8.9\times10^{7}N/m^2$, and tangent modulus 1.28×10^{9} N/m^2.

Two cases were calculated here. The first has a section of 4×8 mm^2 and 5 pairs of ceramic spacers to clamp the coil. The results shows most of deformation is elastic, only a small part is plastic (about 15 um) (see Fig. 2). But on a month and longer basis, the deformation accumulation is considerably big, enough to cause a short with the core if on other measure is taken. The second case is the section of 6×6 mm^2 and 6 pairs of ceramic spacers. The maximum deformation is 11 um, and it is totally elastic, that is, no deformation when the force is removed.

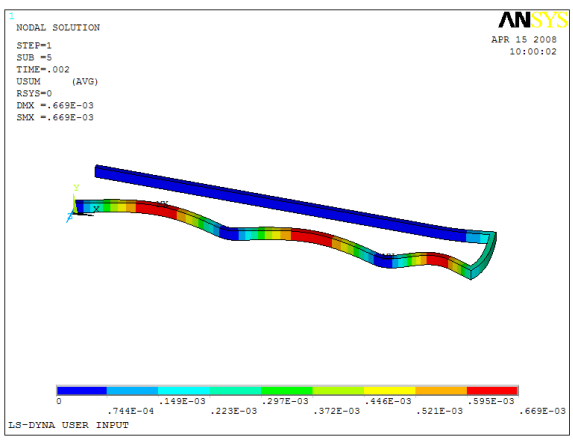

Figure 2: deformation for a coil of section of 4×8 mm^2

Thermal Analysis

The ANSYS electric and thermal coupling analysis was carried out for the coil. Because of the skin effect (the skin depth is 0.7 mm), the resistance of the coil with a section area of 32 mm2 and length 1400 mm is 1.64 mΩ. Given a 5 mΩ contact resistance for the copper braid which connects the coil and the feedthrough, and a 79 A current for the load (rms value of 2 Hz, 60 us half sine with amplitude of 10200 A), the joule heat generation is 4.84e7 W/m3.

The thermal conductivity of the copper coil changes from 401 W/ m·K to 366 W/m·K when the temperature changes from 27 °C to 527 °C; Its specific heat changes from 385 J/kg·K to 417 J/kg·K when the temperature changes from 25 °C to 327 °C; For ceramic, the conductivity and specific heat are not temperature dependent, and the values are 1.46 W/m·K and 790 J/kg·K respectively.

Since there is no convection in the UHV environment, and the radiation is negligible, most of the heat in the coil is dissipated to the air through the feedthrough and vacuum chamber. For boundary condition, two assumptions are given. The first is the temperature of feedthrough ends in the air to be fixed to 45 °C; the second is that in addition to first condition, the temperature for the ceramic sides which contact the magnet copper box to be fixed to 100 °C.

The results show the maximum temperature is about 198 °C for the first assumption, and 134 °C for the second one. In fact, the real maximum temperatures are somewhere in between them.(see Fig. 3).

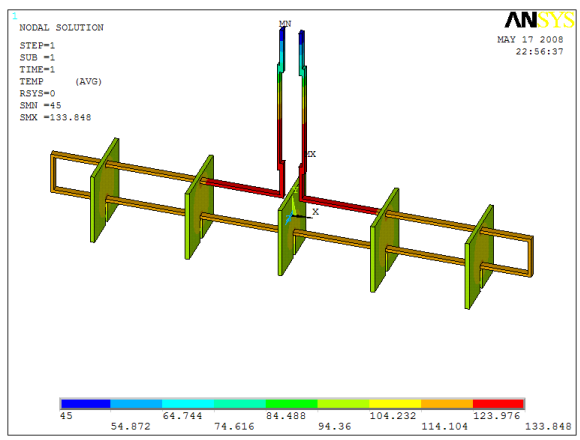

Figure 3: temperature distribution of the coil on the second assumption .

Magnetic Field Analysis

Nonlinear transient eddy-current electromagnetic field analysis was performed on the septum magnets using Opera-2D and Opera-3D (ELEKTRA).

Fig. 4 shows the 2D field distribution at pulse peak when t=30 μs. The main field transverse homogeneity is about ±3.3‰; and there is a time delay between the main field and the leakage field which reaches to its peak at t=~150 μs. The ratio to the main field is around 2.8%

without magnetic shielding screen. When the screen is added, the leakage field is negligible.

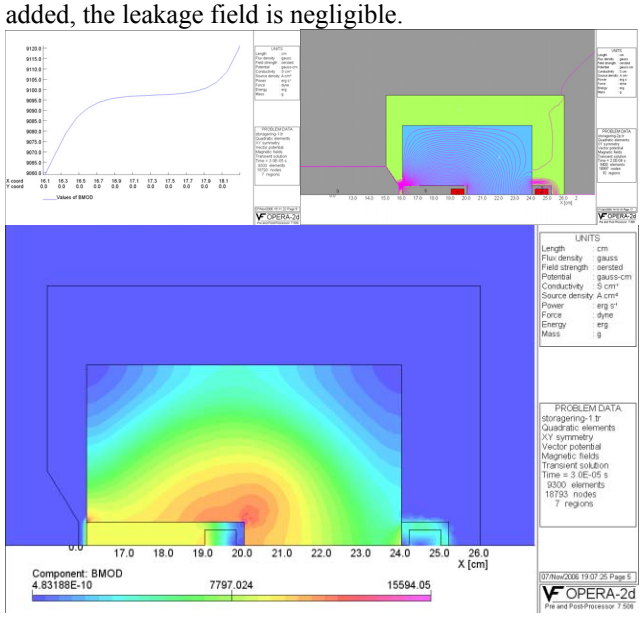

Figure 4: 2D magnetic field distribution; main field transverse homogeneity(upper left); magnetic flux distribution when Mu metal shielding screen is added(upper right)

MAGNETIC MEASUREMENT

The magnetic field measurement was performed on each of the septum magnet for transverse homogeneity, longitudinal profile, effective magnetic length, and integral leakage field versus distance from the septum wall. The measuring equipment consists of "point" coil (4mm in diameter, 20 turns), integral coil (6mm width), and other necessary equipment such as digital integrator oscilloscope and integrator, etc.

The following is the results for Storage Ring Injection septum magnets. Fig. 5 shows time profile of integrated main field (right). From these data we can calculate that the effective magnetic length is 801.45 mm, and the transverse homogeneity of 0.4% for x=2-16 mm (x=0 is the position of septum inner surface).

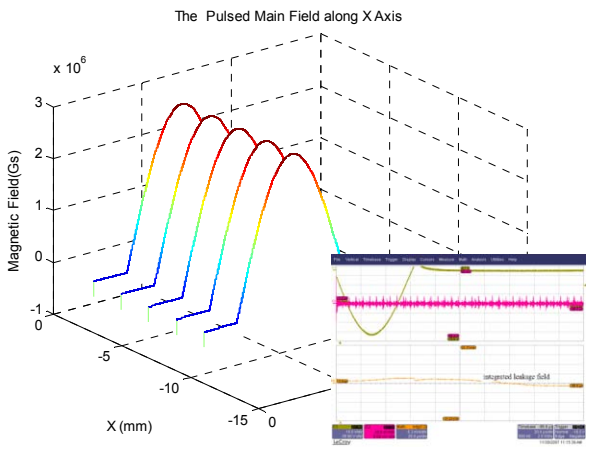

Figure 5: Main field integral profile and leakage field (down right)

Then the measurement of leakage field was performed on Storage Ring injection septum magnets with Mumetal shielding screens. Amazingly any effective leakage field signal cannot be seen at all in the precision range of the LeCroy Wavesurfer 42XS digital integrator oscilloscope. It is safe to say the ratio of integrated leakage field to integrated main field is less than 0.005%.

CONCLUSION

All six in-vacuum eddy current septum magnets were designed, manufactured, tested, and installed in SSRF. In addition to works mentioned above, the magnets position adjustment and alignment were also key procedures to ensure their good performance. High stability and reliability were as important as the good magnetic features. The connection and fixation of the coil to the pulse power supply is something which needs more attentions and carefulness. The commissioning shows that all 6 septum magnets work perfectly.

REFERENCES

[1]Klaus Halbach, Some Thoughts on an Eddy Current Septum Magnet, Argonne National Laboratory and UC Lawrence Berkeley Laboratory

[2]W. Kang, Q. Han, L. Fu, J. Pang, Development of an Eddy-current Septum Magnet for the SSRF Storage Ring, APAC 2001 Proceedings, Beijing China

[3]C. Gough, M. Mailand, Septum and Kicker Systems for the SLS, PAC 2001 proceedings, Chicago, US.